The Astronomical Journal, 168:109 (10pp), 2024 September https://doi.org/10.3847/1538-3881/ad5d76

Resonant and Ultra-short-period Planet Systems Are at Opposite Ends of the Exoplanet Age Distribution

Stephen P. Schmidt[1], Kevin C. Schlaufman[1], and Jacob H. Hamer[2]
[1] William H. Miller III Department of Physics & Astronomy, Johns Hopkins University, 3400 N Charles Street, Baltimore, MD 21218, USA; sschmi42@jh.edu
[2] New Jersey State Museum, 205 W State Street, Trenton, NJ 08608, USA
Received 2024 March 8; revised 2024 June 5; accepted 2024 June 24; published 2024 August 6

Abstract

Exoplanet systems are thought to evolve on secular timescales over billions of years. This evolution is impossible to directly observe on human timescales in most individual systems. While the availability of accurate and precise age inferences for individual exoplanet host stars with ages τ in the interval 1 Gyr $\lesssim \tau \lesssim$ 10 Gyr would constrain this evolution, accurate and precise age inferences are difficult to obtain for isolated field dwarfs like the host stars of most exoplanets. The Galactic velocity dispersion of a thin-disk stellar population monotonically grows with time, and the relationship between age and velocity dispersion in a given Galactic location can be calibrated by a stellar population for which accurate and precise age inferences are possible. Using a sample of subgiants with precise age inferences, we calibrate the age–velocity dispersion relation in the Kepler field. Applying this relation to the Kepler field's planet populations, we find that Kepler-discovered systems plausibly in second-order mean-motion resonances have 1 Gyr $\lesssim \tau \lesssim$ 2 Gyr. The same is true for systems plausibly in first-order mean-motion resonances, but only for systems likely affected by tidal dissipation inside their innermost planets. These observations suggest that many planetary systems diffuse away from initially resonant configurations on secular timescales. Our calibrated relation also indicates that ultra-short-period (USP) planet systems have typical ages in the interval 5 Gyr $\lesssim \tau \lesssim$ 6 Gyr. We propose that USP planets tidally migrated from initial periods in the range 1 day $\lesssim P \lesssim$ 2 days to their observed locations at $P < 1$ day over billions of years and trillions of cycles of secular eccentricity excitation and inside-planet damping.

Unified Astronomy Thesaurus concepts: Exoplanet astronomy (486); Exoplanet dynamics (490); Exoplanet evolution (491); Exoplanet formation (492); Exoplanet migration (2205); Exoplanet systems (484); Exoplanet tides (497); Exoplanets (498); Star-planet interactions (2177); Stellar ages (1581); Stellar kinematics (1608); Tidal interaction (1699)

Materials only available in the online version of record: machine-readable tables

1. Introduction

The long-term evolution of exoplanet systems remains a poorly understood aspect of exoplanet astrophysics, mostly due to the difficulty of accurate and precise age inferences for mature main-sequence stars like most exoplanet hosts. While the occurrence and properties of planetary systems orbiting young stars enable the study of short-term planetary system evolution, studies of the long-term evolution of planetary systems require accurate and precise ages for mature stars. Most stellar age inference methodologies for mature stars like lithium depletion (e.g., Deliyannis et al. 1990), moving group membership (e.g., Barrado y Navascues, D 1998; Barrado y Navascués et al. 1999), gyrochronology (e.g., Barnes 2003, 2007), or stellar activity (e.g., Baliunas et al. 1995) only work for stars no older than a few billion years. New or population-level methods must therefore be used to explore the evolution of exoplanet systems over billions of years.

We have previously used the Galactic velocity dispersions of thin-disk stellar populations to study the evolution of exoplanet systems in several contexts. We showed that short-period hot Jupiters like those discovered by ground-based transit surveys are destroyed by tides while their host stars are on the main sequence and that high-stellar-obliquity hot Jupiter systems are younger than low-stellar-obliquity hot Jupiter systems (Hamer & Schlaufman 2019, 2022). For smaller planets, we argued that ultra-short-period (USP) planets are stable to tidal inspiral and that plausibly resonant systems are relatively young but older than a few hundred million years (Hamer & Schlaufman 2020, 2024). While these results have shown that various exoplanet populations are relatively young or old, to this point we have been unable to obtain characteristic absolute population ages for these planetary systems.

It is now possible to calibrate the age–velocity dispersion relation in the volume of the Galaxy searched for transiting planets by the Kepler space telescope (Borucki et al. 2010), a volume we refer to as the Kepler field. Xiang & Rix (2022) published a catalog of 247,104 ages for subgiants amenable to precise isochrone-based age inference, including 5078 in the Kepler field. Gaia Data Release 3 (DR3; Babusiaux et al. 2023; Gaia Collaboration et al. 2023) provides parallaxes and proper motions for almost every star in the Kepler field. Likewise, the Kepler field has been intensively studied by ground- and space-based spectroscopic surveys, like the California-Kepler Survey (CKS; Johnson et al. 2017; Petigura et al. 2017), the Large Sky Area Multi-Object Fiber Spectroscopic Telescope (LAMOST; Cui et al. 2012; Zhao et al. 2012) Experiment for Galactic Understanding and Exploration (LEGUE; Deng et al. 2012), the Apache Point Observatory Galactic Evolution Experiment (APOGEE; Majewski et al. 2017), and Gaia itself (Katz et al. 2023).

A calibrated age–velocity dispersion relation in the Kepler field would be useful for investigating the secular evolution of small-radius planets in multiple-planet systems. Before Kepler's observations, many systems like these were expected to have experienced convergent type I migration in their parent protoplanetary disks (e.g., Ward 1997) that would have left them in low-order mean-motion resonances (e.g., Terquem & Papaloizou 2007). However, the period ratio distribution observed by Kepler does not exhibit this property (Lissauer et al. 2011; Fabrycky et al. 2014). Numerous ideas to explain Kepler's observation of a lack of systems in low-order mean-motion resonance have been proposed (e.g., Baruteau & Papaloizou 2013; Petrovich et al. 2013; Cui et al. 2021; Charalambous et al. 2022; Laune et al. 2022; Liu et al. 2022). Hamer & Schlaufman (2024) showed that plausibly second-order mean-motion resonant systems are younger than the entire population of multiple-planet systems. The same is true for plausibly first-order mean-motion resonant systems, but only if the innermost planet is likely affected by tidal dissipation. They showed that these two plausibly resonant populations are younger than the multiple-planet population but older than a few hundred million years as indicated by the activity levels and lithium abundances of their host stars. Hamer & Schlaufman (2024) were unable to infer absolute population-level characteristic mean ages τ using their uncalibrated age–velocity dispersion analyses.[3] A calibrated age–velocity dispersion relation would enable the inference of absolute population-level characteristic mean ages for the Kepler field's planet populations.

A calibrated age–velocity dispersion relation would be even more powerful for studies of USP planets. The age of the USP planet population would inform its formation, because USP planet formation models predict a range of ages for the USP planet population. Hamer & Schlaufman (2020) showed that Kepler-discovered USP planets have ages consistent with field stars. In accord with this observation, they argued that USP planets have not recently arrived at their observed locations and therefore are stable against tidal inspiral. This interpretation aligns with "early arrival" theories of USP planet migration (e.g., Lee & Chiang 2017; Petrovich et al. 2019; Li et al. 2020; Millholland & Spalding 2020; Becker et al. 2021; Chen et al. 2022) that advocate for the arrival of USP planets at their observed locations within a few billion years. The Hamer & Schlaufman (2020) observation is also consistent with the possibility that the timescale for USP planets to tidally migrate inward is more than a few billion years, making most USP planets recent arrivals. This migration regime would be possible under the Schlaufman et al. (2010) scenario for USP planet formation in multiple-planet systems, in which proto-USP planets first inwardly migrate via type I migration to their parent protoplanetary disks' magnetospheric truncation radii and then continue inward via tidal migration after disk dissipation due to cycles of secular eccentricity excitation and damping inside the planet.

The absolute characteristic mean age of the USP planet population could differentiate between these possibilities. If USP planets arrive early, as advocated by many authors (e.g., Lee & Chiang 2017; Petrovich et al. 2019; Li et al. 2020; Millholland & Spalding 2020; Becker et al. 2021; Chen et al. 2022), then the characteristic mean age of the USP planet population should be consistent with all Kepler-discovered small planets. On the other hand, if USP planets are recent arrivals, then the characteristic mean age of the USP planet population should be old. If USP planets arrive via tidal migration due to cycles of secular eccentricity excitation and damping inside the planet, then the population of potential proto-USP planets that arrived at their parent protoplanetary disks' magnetospheric truncation radii at orbital periods 1 day $\lesssim P \lesssim$ 2 days should be systematically younger.

In this article, we execute the tests described above. Verifying the Hamer & Schlaufman (2024) result, we find that the characteristic mean ages of plausibly second-order mean-motion resonant systems are older than a few hundred million years but younger than 2 Gyr. The same is true for plausibly first-order resonant systems, but only if the innermost planet is likely affected by tidal dissipation. In contrast, the population of USP planets has a significantly warmer velocity dispersion and a characteristic mean age $5 \lesssim \tau \lesssim 6$ Gyr, both larger than the velocity dispersion and characteristic mean age of the population of proto-USP planets. This suggests that systems with a USP planet are, on average, older than systems with a proto-USP planet and supports the idea that USP planets are recent arrivals at their observed locations. We describe the construction of our samples in Section 2, and our analyses in Section 3. We discuss the implications of our work in Section 4, and summarize our conclusions in Section 5.

2. Data

To study the time evolution of exoplanet systems using the calibrated age–velocity relation, we identify six types of planetary systems. From Hamer & Schlaufman (2024), we obtain samples of multiple-planet systems as well as plausibly first- and second-order mean-motion resonant systems defined using their $\delta_{\rm res}$-based criterion. The Hamer & Schlaufman (2024) $\delta_{\rm res}$ parameter is a modification of the mass- and eccentricity-independent ϵ parameter used by Delisle & Laskar (2014) and Chatterjee & Ford (2015) to describe proximity to resonance that normalizes ϵ by the resonant period ratio to account for the larger "widths" of widely spaced resonances. If we were to instead use the libration width definition in Hamer & Schlaufman (2024) for our first-order resonant sample, we would ultimately find a statistically indistinguishable result. We obtain our sample of USP planet systems from Sanchis-Ojeda et al. (2014). As described in the following paragraph, we also define a sample of proto-USP planet systems.

It is usually assumed that protoplanetary disks are magnetospherically truncated at corotation with their host stars. In that case, the rotation periods of pre-main-sequence stars in star-forming regions can be used to roughly infer the smallest star–planet separations that can result from type I migration. Rebull et al. (2018, 2020) used continuous K2 data to measure rotation periods for solar-mass pre-main-sequence stars with $1 < (V - K_s)_0 < 2$ in Taurus and Upper Sco. They found a median rotation period $P_{\rm rot} = 1.2$ days at 3 Myr in Taurus and $P_{\rm rot} = 2.1$ days at 8 Myr in Upper Sco. Since protoplanetary disks likely dissipate sometime in this age range, these data suggest that the orbital period corresponding to disk magnetospheric truncation radii for solar-mass stars during the epoch of planet formation is in the range 1 day $< P <$ 2 days. We

[3] We use the term "characteristic" to indicate that the ages we obtain for our samples are not calculated as straightforward averages of the individual stellar ages in our samples, but rather that we use samples' galactic velocity dispersions as statistical proxies for entire populations represented by our samples.

therefore define a sample of planets we term proto-USP planets as confirmed planets from the Kepler cumulative planet catalog with planet radii $R_p < 2\,R_\oplus$ and orbital periods $1\,\mathrm{day} < P < 2\,\mathrm{days}$ that would have place them close to their parent protoplanetary disk's magnetospheric truncation radii. We prefer the cumulative Kepler Objects of Interest (KOI) list over the Data Release 25 KOI list due to the extra level of scrutiny provided by the human vetting that produced the cumulative catalog.

To calibrate the age–velocity dispersion relation in the Kepler field, we start with the sample of isochrone-inferred subgiant ages from Xiang & Rix (2022). During the transition from core to shell hydrogen fusion, small changes in mass correspond to large changes in easily observed properties like luminosity or absolute magnitude. As a result, the subgiant phase of stellar evolution permits the most precise isochrone-based age inferences. Xiang & Rix (2022) fit Yonsei-Yale isochrones (Yi et al. 2001; Kim et al. 2002; Yi et al. 2003; Demarque et al. 2004) to the following:

1. Photospheric stellar parameters: effective temperature $T_{\rm eff}$, metallicity [Fe/H], and alpha-to-iron ratio [α/Fe] derived from LAMOST spectroscopy.
2. Gaia Early Data Release 3 (EDR3) parallax-informed absolute magnitudes in Gaia EDR3 $G_{\rm BP}$, G, $G_{\rm RP}$, and 2 Micron All Sky Survey (2MASS) $JHK_{\rm s}$ bands (Skrutskie et al. 2006; Gaia Collaboration et al. 2021).

To limit the Xiang & Rix (2022) sample to the Kepler field, we use the sky position of Kepler's CCDs hosted at STScI's Mikulski Archive for Space Telescopes (MAST).[4] This delivers a sample of 5078 subgiant isochrone-based ages with a median relative precision of 6%, corresponding to a typical absolute age uncertainty of 300 Myr.

To calculate the Galactic velocity dispersion of a sample of stars, we first calculate each star's *UVW* velocities. That calculation requires as inputs parallax, proper motion, and radial velocity. We use the parallaxes and proper motions provided by Gaia DR3.[5] We find that the Gaia EDR3/DR3 source identifiers provided by Xiang & Rix (2022) are missing their last digit. We correct for this by querying the Gaia archive for the 10 possible corrected `source_id`s obtained by appending one digit to each shortened identifier. We then select for each subgiant the Gaia DR3 source that minimizes the on-sky distance between subgiant and Gaia DR3 source. We use this corrected list of Gaia DR3 `source_id` information to query the Gaia archive for the necessary astrometric data. We impose the constraint `parallax_over_error` >10 to ensure high-quality astrometry as well as the common renormalized unit weight error `ruwe` <1.4 data quality cut to exclude to the extent possible the influence of unresolved binaries (e.g., Ziegler et al. 2020; Lindegren et al. 2021a, 2021b). This results in a sample of 5044 Kepler-field subgiants that pass our astrometric data quality cuts.

Radial velocities are also necessary to calculate *UVW* velocities, and we elect to use Gaia DR3 radial velocities as input to our velocity dispersion calculation (Katz et al. 2023). Following Hamer & Schlaufman (2024), we impose the constraints `rv_nb_transits` >10 and `rv_expected_sig_to_noise` >5 to ensure high-quality radial velocities. This procedure results in 3832 subgiants with Gaia astrometry and radial velocities. While there are LAMOST radial velocities available for every star in our sample of subgiants with precise Gaia astrometry and radial velocities, the typical radial velocity measurement precision achieved for LAMOST spectra with spectral resolution $R \approx 1800$ is about $4.3\,\mathrm{km\,s^{-1}}$. On the other hand, the typical radial velocity measurement precision achieved for Gaia Radial Velocity Spectrometer (RVS) spectra with $R \approx 11{,}500$ is about $2.4\,\mathrm{km\,s^{-1}}$. In addition, we find a zero-point offset between these LAMOST and Gaia radial velocity measurements of about $6\,\mathrm{km\,s^{-1}}$.

To determine which of Gaia or LAMOST has the correct zero-point, we use data from APOGEE. We use data derived from spectra that were gathered during the third and fourth phases of the Sloan Digital Sky Survey (SDSS; Eisenstein et al. 2011; Blanton et al. 2017) as part of APOGEE. These spectra were collected with the APOGEE spectrographs (Zasowski et al. 2013, 2017; Wilson et al. 2019; Beaton et al. 2021; Santana et al. 2021) on the New Mexico State University 1 m Telescope (Holtzman et al. 2010) and the Sloan Foundation 2.5 m Telescope (Gunn et al. 2006). As part of SDSS Data Release 17 (Abdurro'uf et al. 2022), these spectra were reduced and analyzed with the APOGEE Stellar Parameter and Chemical Abundance Pipeline (Allende Prieto et al. 2006; Holtzman et al. 2015; Nidever et al. 2015; García Pérez et al. 2016) using a *H*-band line list, MARCS model atmospheres, and model-fitting tools optimized for the APOGEE effort (Alvarez & Plez 1998; Gustafsson et al. 2008; Hubeny & Lanz 2011; Plez 2012; Smith et al. 2013; Cunha et al. 2015; Shetrone et al. 2015; Jönsson et al. 2020; Smith et al. 2021). We find no radial velocity zero-point offsets between Gaia and APOGEE or between Gaia and CKS. We therefore choose to use Gaia radial velocities to characterize the the age–velocity dispersion relation in our subgiant sample.

We follow the same steps described above to calculate the velocity dispersions of our Kepler-discovered planetary system samples. We first obtain Gaia DR3 `source_id` as well as equatorial coordinates, parallaxes, and proper motions for our exoplanet system samples using the 2MASS identifier associated with each Kepler Input Catalog (KIC; Brown et al. 2011) entry and Gaia DR3's `tmass_psc_xsc_best_neighbor` table. We obtain system radial velocities for these samples in descending order of priority from the CKS, APOGEE, and Gaia. For those planet host stars with Gaia RVS-based radial velocities, we apply the same data quality cuts described above. In total, we obtain samples of 60 plausible first-order resonant systems and 60 plausible second-order resonant systems. Our sample of 90 USP planet systems has a median orbital period $P = 0.68$ day and a median planet radius $R_p = 1.21\,R_\oplus$, while our sample of 70 proto-USP planet systems has a median $P = 1.54$ days and a median $R_p = 1.22\,R_\oplus$. For each planet host star in these samples, we report in Table 1 the Kepler and Gaia identifiers, radial velocity with uncertainty and source, and subsample membership.

3. Analysis

We convert equatorial coordinates, proper motions, parallaxes, and radial velocities into Galactic space velocities using the `pyia` package (Price-Whelan 2018). The individual radial

[4] https://archive.stsci.edu/missions/kepler/ffi_footprints/morc_2_ra_dec_4_seasons.txt

[5] For the details of Gaia DR3 and its data processing, see Gaia Collaboration et al. (2016), Lindegren et al. (2021a, 2021b), Fabricius et al. (2021), Gaia Collaboration et al. (2021, 2022, 2023), Marrese et al. (2021, 2022), Riello et al. (2021), Rowell et al. (2021), Torra et al. (2021), and Babusiaux et al. (2023).

Table 1
USP Planet, Proto-USP Planet, and Plausibly/Implausibly Resonant System Samples

Kepler ID	Gaia DR3 source_id	RV (km s^{-1})	RV Source	Sample
1432789	2051748659478657152	-38.8 ± 0.1	APOGEE	Multiple planet
1717722	2051027792165858304	-60.8 ± 0.1	APOGEE	Multiple planet, USP
1718189	2051030231707057024	-26.5 ± 0.1	CKS	Second-order MMR
1718958	2051019683267537024	-24.0 ± 0.1	CKS	Proto-USP
1724719	2051721480924900224	-15.9 ± 0.1	CKS	Multiple planet
1871056	2051738798233021824	-19.2 ± 0.1	CKS	Multiple planet
1996180	2099073667159859840	-4.8 ± 0.1	CKS	Multiple planet
2165002	2051832634677771008	-39.6 ± 0.1	CKS	Multiple planet
2299738	2052587243251659392	-32.9 ± 4.6	Gaia	Proto-USP
2302548	2052528625536778624	-23.5 ± 0.1	CKS	Multiple planet

Notes. Tidally affected first-order resonant systems are included in the sample of all first-order resonant systems, and the Kepler multiple-planet system sample contains all plausibly resonant systems. This table is sorted by KIC ID and is published in its entirety in machine-readable format.

(This table is available in its entirety in machine-readable form in the online article.)

velocity measurement uncertainties are an order of magnitude smaller than our velocity dispersion measurements, so our analyses are not limited by radial velocity precision. We use a Monte Carlo simulation in which `pyia` randomly samples from the Gaia DR3 five-parameter astrometric solution respecting each solution's covariance. It also independently randomly samples radial velocities from a normal distribution with mean and variance as reported in each radial velocity source. We sample 100 realizations from each star's astrometric uncertainty distributions in position, proper motion, parallax, and radial velocity using `pyia`. We then calculate the velocity dispersion σ of each sample,

$$\sigma = \frac{1}{N}\sum_{i=1}^{N}[(U_i - \bar{U})^2 + (V_i - \bar{V})^2 + (W_i - \bar{W})^2]^{\frac{1}{2}}, \quad (1)$$

to construct an ensemble of samples of the entire populations' velocity dispersions.

We use the procedure described above to calculate *UVW* velocities for our sample of subgiants. To generate the age–velocity dispersion relation, we first sort the subgiant sample by age. We calculate the mean age and velocity dispersion in a moving-window sample of 750 subgiants, advance the window by one star, and then repeat until we cover the entire age range of our subgiant sample. For each 750-star window, we obtain 150 bootstrap samples of 750 stars with replacement within the window and calculate the velocity dispersion of each sample. We choose a window of 750 to balance time resolution and velocity dispersion precision. We report the 16th, 50th, and 84th percentiles of the resulting velocity dispersion distributions. In parallel, we calculate the average age of the 750 stars that make up each window. To maximize age resolution at the youngest ages, we use smaller windows. We follow the same procedure described above, but we start each window with the youngest star but sequentially increase the window width from 150 to 750 as the window advances. We use univariate smoothing splines to smooth the curves connecting the 16th, 50th, and 84th percentiles of the velocity dispersion distributions in each window. We plot the results of these calculations in Figures 1 and 2 and report them in tabular form in Table 2.

We use the age–velocity dispersion relation derived above to calculate velocity-dispersion-based characteristic mean ages for the six planet populations represented in Table 1. In particular, we infer lower and upper limits for these characteristic mean ages by identifying the range over which our inferred planet population mean velocity dispersions overlap with the 1σ range of the subgiant-based Kepler-field age–velocity dispersion relation. We do the same for the Kepler-field hot Jupiter and USP planet system samples from Hamer & Schlaufman (2020). We give the resulting characteristic mean age intervals in Table 3.

4. Discussion

We find that plausibly second-order mean-motion resonant and plausibly first-order mean-motion resonant systems likely affected by tidal dissipation discovered by Kepler have characteristic mean ages in the range 0.5 Gyr $\lesssim \tau \lesssim$ 2 Gyr. We also find that USP planet systems discovered by Kepler have characteristic mean ages in the range 4.7 Gyr $\lesssim \tau \lesssim$ 5.8 Gyr, a value offset to older ages than we found for our sample of proto-USP systems 4.1 Gyr $\lesssim \tau \lesssim$ 4.3 Gyr. We emphasize that this is a characteristic mean age, not that there are no young USP planet systems. Indeed, the first USP planet discovered, CoRoT-7 b, appears to be in a relatively young system (Léger et al. 2009; Queloz et al. 2009).

The young characteristic mean ages of plausibly second-order mean-motion resonant and plausibly first-order mean-motion resonant systems likely affected by tidal dissipation supports the hypothesis put forward by Hamer & Schlaufman (2024) that systems of small-radius planets often form resonant and diffuse away from resonances on secular timescales. The absolute ages we infer here provide further evidence against short-timescale explanations for the apparent lack of planet pairs close to low-order mean-motion resonance in the Kepler-discovered period distribution. These short-timescale processes include in situ formation (e.g., Petrovich et al. 2013), interactions between planets and protoplanetary disk density waves caused by outer planets (e.g., Baruteau & Papaloizou 2013; Cui et al. 2021), planet–planet interactions mediated by protoplanetary disk-driven eccentricity damping (e.g., Charalambous et al. 2022; Laune et al. 2022), and progressive protoplanetary disk dissipation-driven disruptions (e.g., Liu et al. 2022). Our inference provides for the first time the characteristic 1 Gyr timescale for the diffusion of initially resonant systems away from resonances.

Our conclusion that the population of USP planets is older than the population we define as proto-USP planets is inconsistent

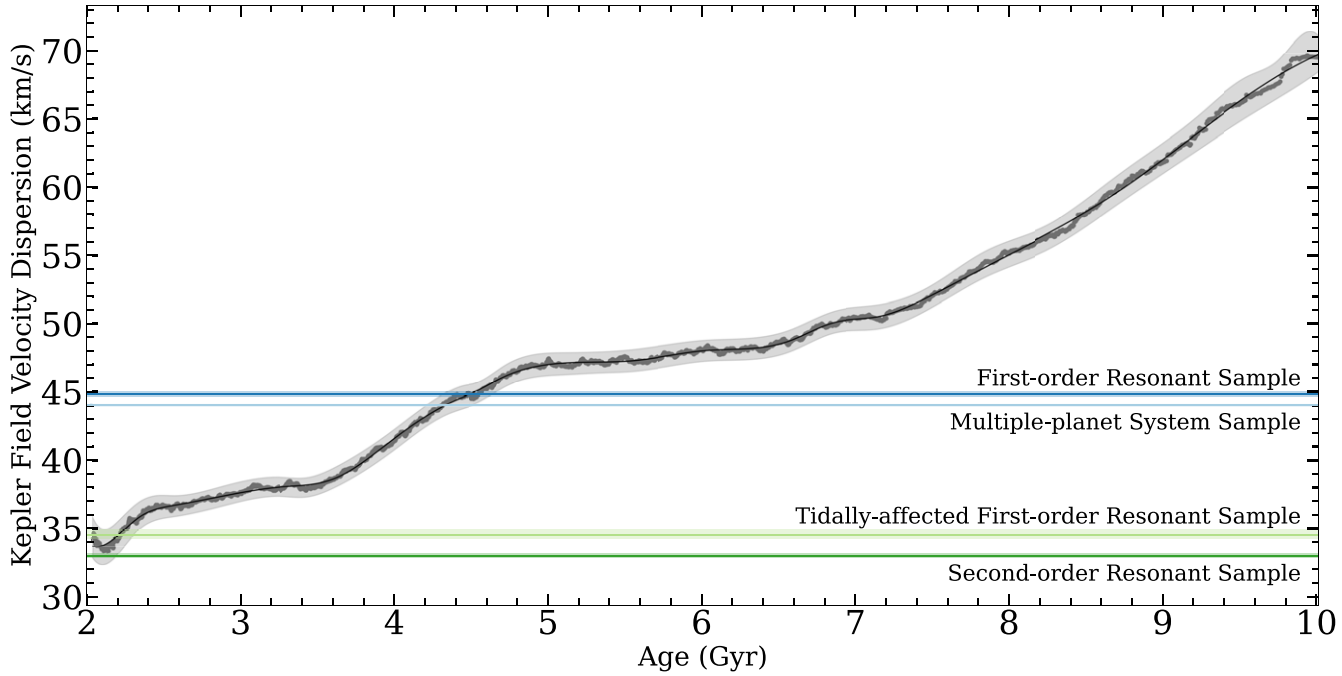

Figure 1. Stellar velocity dispersion as a function of age for the Kepler field. For the sample of subgiants in the Kepler field with ages presented in Xiang & Rix (2022), we first order the sample in age. We then calculate velocity dispersion in consecutive windows of 750 stars and plot the result of these calculations as overlapping dark gray points. We plot as the solid black line a smoothing spline of these data. We plot as the gray polygon the 16th/84th quantile range of the velocity dispersion distribution suggested by bootstrap resampling. We plot as horizontal lines the velocity dispersions of the Hamer & Schlaufman (2024) samples of Kepler-discovered plausibly first- and second-order mean-motion resonant systems as well as the subsample of plausibly first-order resonant systems with an innermost planet affected by tidal dissipation. For comparison, we plot as the light blue horizontal line the velocity dispersion of the complete Hamer & Schlaufman (2024) sample of Kepler-discovered multiple-planet systems. The sample of second-order resonant systems and the subsample of first-order resonant systems with an innermost planet affected by tidal dissipation have characteristic mean ages $\tau \lesssim 2$ Gyr. On the other hand, the overall sample of first-order resonant systems has a similar velocity dispersion and therefore age as the complete sample of Kepler-discovered multiple-planet systems. Combined with the Hamer & Schlaufman (2024) observation that the characteristic mean ages of these resonant populations are older than 500 Myr, the implication is that many multiple-planet systems form in mean-motion resonances and diffuse away from resonance over about 1 Gyr.

with USP planet formation models in which USP planets arrive at their observed locations in less than about 1 Gyr. We rule out USP planet formation mechanisms that take place while protoplanetary disks are present, like the scenario advocated by Becker et al. (2021) as a consequence of protostellar outburst-driven accretion events. Our observations are likewise inconsistent with USP planet formation as a consequence of the gravitational influence of an oblate host star's J_2 quadrupolar potential (Li et al. 2020; Chen et al. 2022), as that scenario requires USP planets to have arrived at their observed locations in less than 1 Gyr. Obliquity-tide-driven migration is also expected to have a timescale shorter than 1 Gyr (Millholland & Spalding 2020).

Though eccentricity-excitation-driven migration has been a frequent explanation for USP planet formation, different models predict a range of migration timescales. In general, a small number of large-amplitude eccentricity excitations will lead to short migration timescales (e.g., Petrovich et al. 2019). These short migration timescales are disfavored by our conclusion that USP planets take many billions of years to arrive at their observed locations. On the other hand, frequent cycles of low-amplitude eccentricity excitation will lead to long migration timescales that are consistent with our observations (e.g., Schlaufman et al. 2010). Tidal migration resulting from the dissipation of orbital energy in an especially dissipative host star would also be consistent with our observations (e.g., Lee & Chiang 2017).

To investigate the plausibility of the scenario that proto-USP planets tidally migrate to become USP planets due to cycles of eccentricity excitation and dissipation, we integrate the coupled system of ordinary differential equations (ODEs) modeling the tidal evolution process presented in Leconte et al. (2010). This system of ODEs is based on the complete tidal evolution equations of the Hut (1981) model and valid at any order in eccentricity, obliquity, and spin. For the host star of our model system, we use the self-consistent rotational stellar evolution model for a $M_* = 1\,M_\odot$, solar-composition, median-rotating star presented in Amard et al. (2019). The median USP planet in our sample has planet radius $R_\mathrm{p} = 1.2\,R_\oplus$, corresponding to a planet mass $M_\mathrm{p} = 2.0\,M_\oplus$ assuming the Zeng et al. (2019) mass–radius relation for an Earth-like composition. We assume the system begins its post protoplanetary disk dissipation evolution with eccentricity $e = 0.1$ at $a = 0.030$ au, corresponding to $P = 1.9$ days. We further assume that the planet has a specific tidal quality factor $Q_\mathrm{p}{}' = 10^2$, its host star has a stellar tidal quality factor $Q_*{}' = 10^7$, and the system's eccentricity cannot fall below a nonzero but still unobservably small value $e = 0.005$. Under these conditions, the planet reaches a period $P < 1$ day in 5 Gyr, a timescale consistent with our observational result. We plot the result of this calculation in Figure 3. We expect ohmic dissipation to have a negligible effect on the orbital evolution of the planet, as the amount of orbital energy dissipated in this way is much, much less than the amount of orbital energy dissipated through tides (e.g., Wu & Lithwick 2013).

As $Q_\mathrm{p}{}'$ is sensitive to interior structure and tidal forcing frequency (Tobie et al. 2019), it may vary from our assumed value $Q_\mathrm{p}{}' = 10^2$ within the range $80 < Q_\mathrm{p}{}' < 280$. This

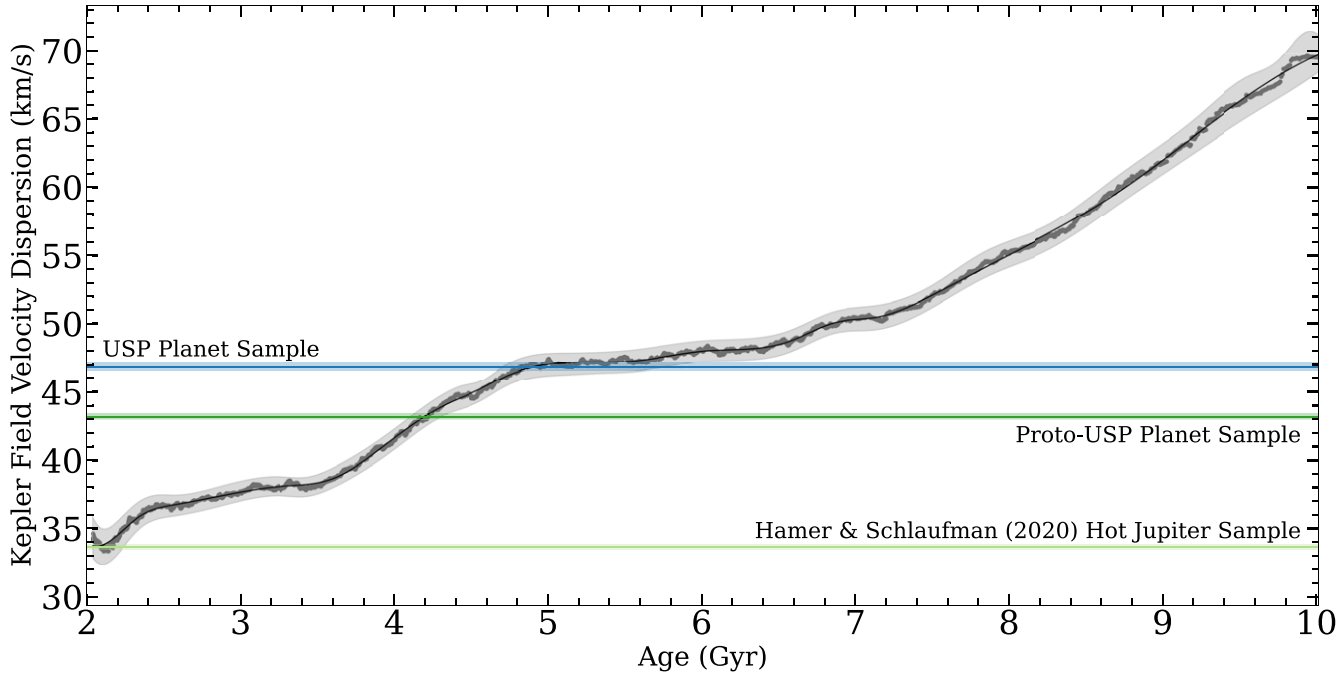

Figure 2. Stellar velocity dispersion as a function of age for the Kepler field. The age–velocity dispersion relation is the same as in Figure 1. We plot as horizontal lines the velocity dispersions of the Hamer & Schlaufman (2020) sample of Kepler-discovered hot Jupiter systems as well as our sample of USP planet systems. We define proto-USP planets as confirmed planets from the Kepler cumulative planet catalog with planet radii $R_p < 2\ R_\oplus$ and orbital periods 1 day $< P <$ 2 days, and we plot as the dark green horizontal line that sample's velocity dispersion. Our USP planet system sample has a characteristic mean age 4.7 Gyr $\lesssim \tau \lesssim$ 5.8 Gyr, while the proto-USP planet sample has a characteristic mean age 4.1 Gyr $\lesssim \tau \lesssim$ 4.3 Gyr. We argue that the best explanation for this age offset is that USP planets tidally migrated from longer-period orbits due to cycles of secular eccentricity excitation and tidal damping in multiple-planet systems.

Table 2
Kepler-field Age–Velocity Dispersion Relation

Window Average Age (Gyr)	Lower Uncertainty (km s^{-1})	Velocity Dispersion (km s^{-1})	Upper Uncertainty (km s^{-1})
2.04007	1.35312	34.17309	1.58540
2.04181	1.21826	34.28341	1.22931
2.04354	1.29945	34.62238	1.51263
2.04525	1.50722	34.53612	1.30693
2.04695	1.58769	34.56045	1.53181
2.04868	1.52845	34.46360	1.48397
2.05040	1.20451	34.35825	1.22901
2.05210	1.54166	34.30429	1.42783
2.05380	1.49620	34.34044	1.71104
2.05549	1.37817	34.26295	1.35232

Notes. This table is ordered by average age in ascending order and is published in its entirety in machine-readable format. Upper uncertainty refers to the difference between the 84th and 50th percentiles, and the lower uncertainty refers to the difference between the 50th and 16th percentiles.

(This table is available in its entirety in machine-readable form in the online article.)

interval is bounded below by measurements of Q_p' for Mars (Lainey et al. 2007, 2021) and above by predictions for Earth's Q_p' if it lacked oceans (Ray et al. 2001). This range of possible values could lead to migration timescales that differ by up to a factor of 2 (i.e., a few billion years), as da/dt from Leconte et al. (2010) is linear in Q_p'. Likewise, changes of 0.001 to the system's minimum eccentricity would lead to a similar lengthening or shortening of its migration timescale. We emphasize that in addition to a range of possible Q_p', the excited eccentricity is not a precisely known quantity but rather an empirical choice to match our observation.

We also argue that the minimum eccentricity we assumed in our model as a consequence of secular eccentricity oscillations in multiple-planet systems is also plausible. We use the `celmech` code (Hadden & Tamayo 2022) to study the secular behavior of USP planet systems resembling the USP systems with additional, longer-period transiting planets identified by Sanchis-Ojeda et al. (2014).[6] In the absence of tidal dissipation, the secular eccentricity excitation caused by planets exterior to a proto-USP planet are predicted to easily be large enough to sustain the excited eccentricity we assume in our calculations. The self-consistent calculation of the eccentricity excitation and tidal dissipation in an N-body model of a proto-USP planet system over the necessary timescales is computationally expensive and much more complicated. We suggest that such a calculation should be the subject of future investigation.

Our preferred model relies on a sustained, very small, but nonzero eccentricity that will be very hard to measure for a USP or proto-USP planet system. While Doppler measurements lack the necessary precision, the precise timing of transits and secondary eclipses could in principle result in a more attainable observational eccentricity constraint for a USP planet system. Full orbits of several USP planets orbiting solar-type host stars have been or are currently scheduled for observation by the JWST in Cycles 1 or 2, including K2-22 b (Sanchis-Ojeda et al. 2015), K2-141 b (Malavolta et al. 2018), and TOI-561 b (Lacedelli et al. 2021). To evaluate the eccentricity constraints that may be possible with these observations, we use Equation (6) from Wallenquist (1950)

[6] These systems are Kepler-10, Kepler-487, Kepler-607, Kepler-990, Kepler-1315, Kepler-1322, Kepler-1813, Kepler-1814, Kepler-1834, and Kepler-1977.

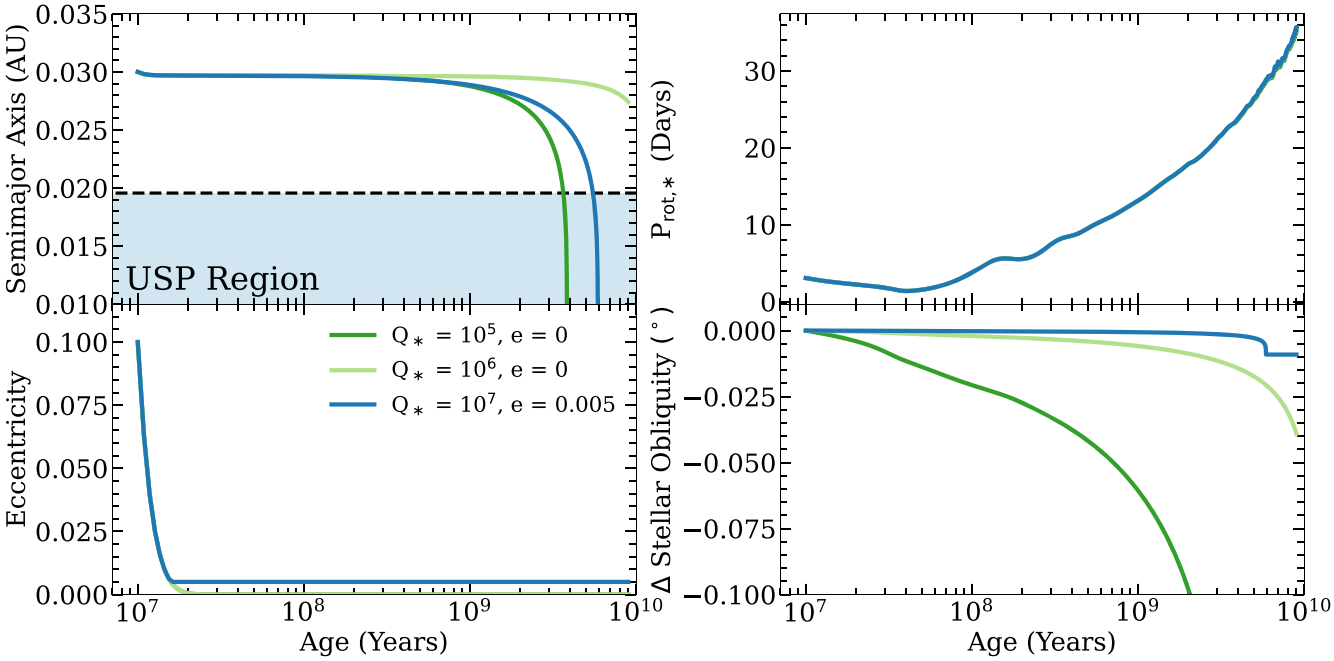

Figure 3. Model for the self-consistent tidal evolution of a typical USP planet system. We plot as colored lines the semimajor axis (top left), eccentricity (bottom left), stellar rotation period (top right), and difference in stellar obliquity from the initial value of 20° (bottom right) as functions of time in years. Our model uses the system of ODEs presented in Leconte et al. (2010) that solves the coupled tidal evolution of the rotation and revolution of both a planet and its host star. We account for the rotational evolution of the host star due to stellar evolution and winds using a solar-composition, median-rotation $M_* = 1\ M_\odot$ stellar model from the rotational stellar evolution grid presented in Amard et al. (2019). We model the median USP planet with $R_p = 1.2\ R_\oplus$, $2.0\ M_\oplus$, and $Q_p' = 10^2$. We plot in blue the solution with an assumed stellar tidal quality factor $Q_*' = 10^7$ as appropriate for solar-type main-sequence stars (Barker 2020) and a nonzero but unobservable excited eccentricity $e = 0.005$. Given these parameters, the rotation and revolution of the planet are quickly synchronized and the planetary obliquity is quickly damped (e.g., Leconte et al. 2010). To evaluate whether tidal dissipation in the star could reproduce our observational result, we plot as dark and light green lines models calculated using the same ODE system, but with no eccentricity excitation and smaller $Q_*' = 10^6$ (light green) and $Q_*' = 10^5$ (dark green). This model corroborates our observational evidence that it takes billions of years and trillions of orbits for a rocky planet to tidally migrate and become a USP planet as a consequence of tidal dissipation inside the planet.

Table 3
Velocity Dispersions for Exoplanet Populations in the Kepler Field

Sample	Number of Systems	Velocity Dispersion (km s^{-1})	Age Range (Gyr)	Source
Ultra-short-period planet systems	68	$47.0^{+0.1}_{-0.1}$	(4.7, 5.9)	Hamer & Schlaufman (2020)
Hot Jupiter systems	24	$33.6^{+0.2}_{-0.2}$	<2.2	Hamer & Schlaufman (2020)
Ultra-short-period planet systems	90	$46.8^{+0.3}_{-0.2}$	(4.7, 5.8)	This work
Proto-ultra-short-period planet systems	70	$43.2^{+0.2}_{-0.2}$	(4.1, 4.3)	This work
Multiple-planet systems	563	$44.0^{+0.1}_{-0.1}$	(4.2, 4.5)	This work
Plausibly first-order resonant systems	60	$44.8^{+0.2}_{-0.1}$	(4.3, 4.6)	This work
Plausibly second-order resonant systems	60	$33.0^{+0.1}_{-0.1}$	(0.5, 2.2)	This work
Tidally affected plausibly first-order resonant systems	9	$34.5^{+0.3}_{-0.2}$	(0.5, 2.3)	This work

for the tangential component of the eccentricity:

$$e\cos\omega = \frac{\pi}{P}\left(\frac{t_2 - t_1 - P/2}{1 + \csc^2 i}\right), \quad (2)$$

where e, ω, P, and i are the system's eccentricity, argument of periastron, orbital period, and inclination. The quantity t_2–t_1 is the time difference between the transit and eclipse midpoints. In the ideal situation where e is entirely tangential (i.e., $\cos\omega = 1$), robust measurements would require eccentricity inference precisions of about 0.001. In systems with $i < 89.9°$, eccentricity uncertainties are always larger than inclination uncertainties so inclination uncertainties will be the limiting factors for eccentricity inferences. To this point, inclination uncertainties for the best-characterized USP planet systems have always been larger than 0.1° (e.g., Fogtmann-Schulz et al. 2014; Stassun et al. 2017; Vanderburg et al. 2017; Bourrier et al. 2018; Brinkman et al. 2023). This is also the case for the larger sample of Sanchis-Ojeda et al. (2014) Kepler discoveries that has a median inclination uncertainty of 3.5°. The net result is that the sustained eccentricity necessary for our tidal migration scenario is at present too small to be observed.

Our conclusion that the characteristic mean age 4.7 Gyr $\lesssim \tau \lesssim$ 5.8 Gyr of the population of Kepler-discovered USP planets can also in principle be explained by the USP planet formation scenario invoking tidal dissipation inside host stars

advocated by Lee & Chiang (2017) if protoplanetary disks are truncated at $P \lesssim 1$ day. The analyses presented in that article relied on hypothesized disk magnetospheric truncation radii inferred from ground-based stellar rotation periods for young stars in the Orion Nebular Cluster, NGC 2362, and NGC 2547. Those rotation periods were derived from ground-based observations that, while sensitive to the large-amplitude variations typical of young, low-mass star light curves, were likely insensitive to the small-amplitude variations typical of young, solar-mass star light curves. Rotation periods based on ground-based data are also susceptible to aliasing with the 1 day observing cadence of all single-location ground-based observations. The sample of rotation periods for stars in the mass range $0.5\,M_{\odot} < M_{*} < 1.4\,M_{\odot}$ shown in Figure 2 of Lee & Chiang (2017) are almost certainly biased toward the low-mass end of that mass range because lower-mass stars are both more numerous and have larger-amplitude variations in their light curves more easily detected in ground-based data. They may also be aliased to $P_{\rm rot} = 1$ day because of observing cadence.

As we argued in Section 2, continuous space-based K2 observations of Taurus and Upper Sco analyzed in Rebull et al. (2018, 2020) suggest that disks around solar-mass protostars are truncated somewhere in the range 1 day $\lesssim P \lesssim$ 2 day. To evaluate the Lee & Chiang (2017) scenario in light of these new data, we again solve the Leconte et al. (2010) system of ODEs assuming the same stellar and planet properties but with two changes: We allow the system's eccentricity to go to zero and vary the stellar specific tidal quality factor Q_{*}'. We find that in this case a proto-USP planet can evolve into a USP planet in 5 Gyr only when its host star has $Q_{*}' \sim 10^{5}$, about an order of magnitude smaller (i.e., more dissipative) than predicted by theoretical models in this planet mass, stellar mass, and orbital period range (e.g., Ogilvie & Lin 2007; Barker 2020; Weinberg et al. 2024). We plot this calculation for both $Q_{*}' = 10^{5}$ and $Q_{*}' = 10^{6}$ in Figure 3. Unless stars are significantly more dissipative than expected with a typical $Q_{*}' \approx 2 \times 10^{5}$, then the scenario in which proto-USP planets start at their parent protoplanetary disk's magnetospheric truncation radii and migrate inward due to tidal dissipation inside their host star is inconsistent with our observations.

The stellar tidal quality factor required for tidal dissipation inside a proto-USP planet's host star to explain our observation is similar to the measured value $Q_{*}' \approx 2 \times 10^{5}$ for WASP-12 (Maciejewski et al. 2016; Patra et al. 2017; Yee et al. 2020; Turner et al. 2021), the only plausibly main-sequence star with a directly inferred Q_{*}' value.[7] However, WASP-12's current Q_{*}' lies at the lower end of the range of Q_{*}' inferred for hot Jupiter host stars (e.g., Jackson et al. 2008; Lanza et al. 2011; Husnoo et al. 2012; Adams et al. 2024). In addition, a hot Jupiter system's orbital period, host-star structure, and planet mass have been theoretically shown to affect Q_{*}' (e.g., Weinberg et al. 2012, 2024). These models suggest that the Q_{*}' for WASP-12 is at least an order of magnitude smaller (i.e., more dissipative) than for the host stars of our USP and proto-USP planet samples. It is also plausible that WASP-12 is a subgiant and consequently more dissipative than the main-sequence host stars in our samples (Weinberg et al. 2017; Bailey & Goodman 2019). We therefore argue that the value of Q_{*}' inferred for the WASP-12 system is not representative of the host stars in our USP and proto-USP planet samples.

[7] Kepler-1658 b has also been shown to be experiencing orbital decay (Vissapragada et al. 2022), but its host star is unambiguously a subgiant.

5. Conclusion

We find that the population of Kepler-discovered multiple-planet systems has a characteristic mean age 4.2 Gyr $\lesssim \tau \lesssim$ 4.5 Gyr. On the other hand, the population of Kepler-discovered plausibly second-order mean-motion resonant planetary systems has a characteristic mean age in the range 0.5 Gyr $\lesssim \tau \lesssim$ 2 Gyr. The same is true for Kepler-discovered plausibly first-order mean-motion resonant planetary systems, but only for systems likely affected by tidal dissipation inside their innermost planets. We conclude that many planetary systems form in resonance and then diffuse away from resonance with a characteristic timescale of 1 Gyr. We show that the population of Kepler field USP planet systems has a characteristic mean age 4.7 Gyr $\lesssim \tau \lesssim$ 5.8 Gyr that is older than the characteristic mean age of the population of proto-USP planets 4.1 Gyr $\lesssim \tau \lesssim$ 4.3 Gyr. The older age of USP planets suggests that they have only recently arrived at their observed locations, an observation that is inconsistent with models of USP planet formation in which USP planets arrive at $P \lesssim 1$ day in less than 1 Gyr. Among the range of models proposed for USP planet formation, we suggest that the formation of USP planets via tidal migration from initial periods in the range 1 day $\lesssim P \lesssim$ 2 day to their observed locations at $P < 1$ day as a consequence of billions of years and trillions of cycles of secular eccentricity excitation and tidal damping inside the tidally migrating planet is most consistent with the available data.

Acknowledgments

We thank Colin Norman, Sam Grunblatt, Daniel Thorngren, and David Sing for helpful insight about our findings. This material is based upon work supported by the National Science Foundation under grant No. 2009415. This work has made use of data from the European Space Agency (ESA) mission Gaia (https://www.cosmos.esa.int/gaia), processed by the Gaia Data Processing and Analysis Consortium (DPAC; https://www.cosmos.esa.int/web/gaia/dpac/consortium). Funding for the DPAC has been provided by national institutions, in particular the institutions participating in the Gaia Multilateral Agreement. This research has made use of the SIMBAD database, operated at CDS, Strasbourg, France (Wenger et al. 2000). This research has made use of the VizieR catalog access tool, CDS, Strasbourg, France. The original description of the VizieR service was published in Ochsenbein et al. (2000). This research has made use of the NASA Exoplanet Archive (Akeson et al. 2013), which is operated by the California Institute of Technology, under contract with the National Aeronautics and Space Administration under the Exoplanet Exploration Program. Funding for SDSS-III has been provided by the Alfred P. Sloan Foundation, the Participating Institutions, the National Science Foundation, and the U.S. Department of Energy Office of Science. The SDSS-III website is http://www.sdss3.org/. SDSS-III is managed by the Astrophysical Research Consortium for the Participating Institutions of the SDSS-III Collaboration including the University of Arizona, the Brazilian Participation Group, Brookhaven National Laboratory, Carnegie Mellon University, University of Florida, the French Participation Group, the German Participation Group, Harvard University, the Instituto de Astrofisica de Canarias, the Michigan State/Notre Dame/JINA Participation Group, Johns Hopkins University, Lawrence Berkeley National Laboratory, Max Planck

Institute for Astrophysics, Max Planck Institute for Extraterrestrial Physics, New Mexico State University, New York University, Ohio State University, Pennsylvania State University, University of Portsmouth, Princeton University, the Spanish Participation Group, University of Tokyo, University of Utah, Vanderbilt University, University of Virginia, University of Washington, and Yale University. Funding for the Sloan Digital Sky Survey IV has been provided by the Alfred P. Sloan Foundation, the U.S. Department of Energy Office of Science, and the participating institutions. SDSS-IV acknowledges support and resources from the Center for High Performance Computing at the University of Utah. The SDSS website is http://www.sdss4.org. SDSS-IV is managed by the Astrophysical Research Consortium for the Participating Institutions of the SDSS Collaboration including the Brazilian Participation Group, the Carnegie Institution for Science, Carnegie Mellon University, Center for Astrophysics | Harvard & Smithsonian, the Chilean Participation Group, the French Participation Group, Instituto de Astrofísica de Canarias, The Johns Hopkins University, Kavli Institute for the Physics and Mathematics of the Universe (IPMU)/University of Tokyo, the Korean Participation Group, Lawrence Berkeley National Laboratory, Leibniz Institut für Astrophysik Potsdam (AIP), Max-Planck-Institut für Astronomie (MPIA Heidelberg), Max-Planck-Institut für Astrophysik (MPA Garching), Max-Planck-Institut für Extraterrestrische Physik (MPE), National Astronomical Observatories of China, New Mexico State University, New York University, University of Notre Dame, Observatário Nacional / MCTI, The Ohio State University, Pennsylvania State University, Shanghai Astronomical Observatory, the United Kingdom Participation Group, Universidad Nacional Autónoma de México, University of Arizona, University of Colorado Boulder, University of Oxford, University of Portsmouth, University of Utah, University of Virginia, University of Washington, University of Wisconsin, Vanderbilt University, and Yale University. This paper includes data collected by the Kepler mission and obtained from the MAST data archive at the Space Telescope Science Institute (STScI). Funding for the Kepler mission is provided by the NASA Science Mission Directorate. STScI is operated by the Association of Universities for Research in Astronomy, Inc., under NASA contract NAS 5-26555. This research has made use of NASA's Astrophysics Data System.

Facilities: ADS, CDS, Exoplanet Archive, Gaia, Kepler, MAST, Sloan.

Software: astropy (Astropy Collaboration et al. 2013, 2018, 2022), `celmech` (Hadden & Tamayo 2022), `matplotlib` (Hunter 2007), `numpy` (Harris et al. 2020), `pandas` (pandas development team, T 2020; Wes McKinney 2010), `pyia` (Price-Whelan 2018), `scipy` (Virtanen et al. 2020), `TOPCAT` (Taylor 2005).

ORCID iDs

Stephen P. Schmidt https://orcid.org/0000-0001-8510-7365
Kevin C. Schlaufman https://orcid.org/0000-0001-5761-6779
Jacob H. Hamer https://orcid.org/0000-0002-7993-4214

References

Abdurro'uf, A. K., Aerts, C., et al. 2022, ApJS, 259, 35
Adams, E. R., Jackson, B., Sickafoose, A. A., et al. 2024, PSJ, 5, 163
Akeson, R. L., Chen, X., Ciardi, D., et al. 2013, PASP, 125, 989
Allende Prieto, C., Beers, T. C., Wilhelm, R., et al. 2006, ApJ, 636, 804
Alvarez, R., & Plez, B. 1998, A&A, 330, 1109
Amard, L., Palacios, A., Charbonnel, C., et al. 2019, A&A, 631, A77
Astropy Collaboration, Robitaille, T. P., Tollerud, E. J., et al. 2013, A&A, 558, A33
Astropy Collaboration, Price-Whelan, A. M., Sipőcz, B. M., et al. 2018, AJ, 156, 123
Astropy Collaboration, Price-Whelan, A. M., Lim, P. L., et al. 2022, ApJ, 935, 167
Babusiaux, C., Fabricius, C., Khanna, S., et al. 2023, A&A, 674, A32
Bailey, A., & Goodman, J. 2019, MNRAS, 482, 1872
Baliunas, S. L., Donahue, R. A., Soon, W. H., et al. 1995, ApJ, 438, 269
Barker, A. J. 2020, MNRAS, 498, 2270
Barnes, S. A. 2003, ApJ, 586, 464
Barnes, S. A. 2007, ApJ, 669, 1167
Barrado y Navascues, D. 1998, A&A, 339, 831
Barrado y Navascués, D., Stauffer, J. R., Song, I., & Caillault, J. P. 1999, ApJL, 520, L123
Baruteau, C., & Papaloizou, J. C. B. 2013, ApJ, 778, 7
Beaton, R. L., Oelkers, R. J., Hayes, C. R., et al. 2021, AJ, 162, 302
Becker, J. C., Batygin, K., & Adams, F. C. 2021, ApJ, 919, 76
Blanton, M. R., Bershady, M. A., Abolfathi, B., et al. 2017, AJ, 154, 28
Borucki, W. J., Koch, D., Basri, G., et al. 2010, Sci, 327, 977
Bourrier, V., Dumusque, X., Dorn, C., et al. 2018, A&A, 619, A1
Brinkman, C. L., Weiss, L. M., Dai, F., et al. 2023, AJ, 165, 88
Brown, T. M., Latham, D. W., Everett, M. E., & Esquerdo, G. A. 2011, AJ, 142, 112
Charalambous, C., Teyssandier, J., & Libert, A. S. 2022, MNRAS, 514, 3844
Chatterjee, S., & Ford, E. B. 2015, ApJ, 803, 33
Chen, C., Li, G., & Petrovich, C. 2022, ApJ, 930, 58
Cui, X.-Q., Zhao, Y.-H., Chu, Y.-Q., et al. 2012, RAA, 12, 1197
Cui, Z., Papaloizou, J. C. B., & Szuszkiewicz, E. 2021, ApJ, 921, 142
Cunha, K., Smith, V. V., Johnson, J. A., et al. 2015, ApJL, 798, L41
Delisle, J. B., & Laskar, J. 2014, A&A, 570, L7
Deliyannis, C. P., Demarque, P., & Kawaler, S. D. 1990, ApJS, 73, 21
Demarque, P., Woo, J.-H., Kim, Y.-C., & Yi, S. K. 2004, ApJS, 155, 667
Deng, L.-C., Newberg, H. J., Liu, C., et al. 2012, RAA, 12, 735
Eisenstein, D. J., Weinberg, D. H., Agol, E., et al. 2011, AJ, 142, 72
Fabricius, C., Luri, X., Arenou, F., et al. 2021, A&A, 649, A5
Fabrycky, D. C., Lissauer, J. J., Ragozzine, D., et al. 2014, ApJ, 790, 146
Fogtmann-Schulz, A., Hinrup, B., Van Eylen, V., et al. 2014, ApJ, 781, 67
Gaia Collaboration, Prusti, T., de Bruijne, J. H. J., et al. 2016, A&A, 595, A1
Gaia Collaboration, Brown, A. G. A., Vallenari, A., et al. 2021, A&A, 649, A1
Gaia Collaboration, Klioner, S. A., Lindegren, L., et al. 2022, A&A, 667, A148
Gaia Collaboration, Vallenari, A., Brown, A. G. A., et al. 2023, A&A, 674, A1
García Pérez, A. E., Allende Prieto, C., Holtzman, J. A., et al. 2016, AJ, 151, 144
Gunn, J. E., Siegmund, W. A., Mannery, E. J., et al. 2006, AJ, 131, 2332
Gustafsson, B., Edvardsson, B., Eriksson, K., et al. 2008, A&A, 486, 951
Hadden, S., & Tamayo, D. 2022, AJ, 164, 179
Hamer, J. H., & Schlaufman, K. C. 2019, AJ, 158, 190
Hamer, J. H., & Schlaufman, K. C. 2020, AJ, 160, 138
Hamer, J. H., & Schlaufman, K. C. 2022, AJ, 164, 26
Hamer, J. H., & Schlaufman, K. C. 2024, AJ, 167, 55
Harris, C. R., Millman, K. J., van der Walt, S. J., et al. 2020, Natur, 585, 357
Holtzman, J. A., Harrison, T. E., & Coughlin, J. L. 2010, AdAst, 2010, 193086
Holtzman, J. A., Shetrone, M., Johnson, J. A., et al. 2015, AJ, 150, 148
Hubeny, I., & Lanz, T. 2011, Synspec: General Spectrum Synthesis Program, Astrophysics Source Code Library., ascl:1109.022
Hunter, J. D. 2007, CSE, 9, 90
Husnoo, N., Pont, F., Mazeh, T., et al. 2012, MNRAS, 422, 3151
Hut, P. 1981, A&A, 99, 126
Jackson, B., Greenberg, R., & Barnes, R. 2008, ApJ, 678, 1396
Johnson, J. A., Petigura, E. A., Fulton, B. J., et al. 2017, AJ, 154, 108
Jönsson, H., Holtzman, J. A., Allende Prieto, C., et al. 2020, AJ, 160, 120
Katz, D., Sartoretti, P., Guerrier, A., et al. 2023, A&A, 674, A5
Kim, Y.-C., Demarque, P., Yi, S. K., & Alexander, D. R. 2002, ApJS, 143, 499
Lacedelli, G., Malavolta, L., Borsato, L., et al. 2021, MNRAS, 501, 4148
Lainey, V., Dehant, V., & Pätzold, M. 2007, A&A, 465, 1075
Lainey, V., Pasewaldt, A., Robert, V., et al. 2021, A&A, 650, A64
Lanza, A. F., Damiani, C., & Gandolfi, D. 2011, A&A, 529, A50
Laune, J. T., Rodet, L., & Lai, D. 2022, MNRAS, 517, 4472
Leconte, J., Chabrier, G., Baraffe, I., & Levrard, B. 2010, A&A, 516, A64
Lee, E. J., & Chiang, E. 2017, ApJ, 842, 40
Léger, A., Rouan, D., Schneider, J., et al. 2009, A&A, 506, 287
Li, G., Dai, F., & Becker, J. 2020, ApJL, 890, L31
Lindegren, L., Bastian, U., Biermann, M., et al. 2021a, A&A, 649, A4

Lindegren, L., Klioner, S. A., Hernández, J., et al. 2021b, A&A, 649, A2
Lissauer, J. J., Ragozzine, D., Fabrycky, D. C., et al. 2011, ApJS, 197, 8
Liu, B., Raymond, S. N., & Jacobson, S. A. 2022, Natur, 604, 643
Maciejewski, G., Dimitrov, D., Fernández, M., et al. 2016, A&A, 588, L6
Majewski, S. R., Schiavon, R. P., Frinchaboy, P. M., et al. 2017, AJ, 154, 94
Malavolta, L., Mayo, A. W., Louden, T., et al. 2018, AJ, 155, 107
Marrese, P. M., Marinoni, S., Fabrizio, M., & Altavilla, G. 2021, Gaia EDR3 Documentation, European Space Agency
Marrese, P. M., Marinoni, S., Fabrizio, M., & Altavilla, G. 2022, Gaia DR3 Documentation, European Space Agency
McKinney, W. 2010, in Proc, of the 9th Python in Science Conf., ed. Stéfan van der Walt & Jarrod Millman (Austin, TX: SciPy), 61
Millholland, S. C., & Spalding, C. 2020, ApJ, 905, 71
Nidever, D. L., Holtzman, J. A., Allende Prieto, C., et al. 2015, AJ, 150, 173
Ochsenbein, F., Bauer, P., & Marcout, J. 2000, A&AS, 143, 23
Ogilvie, G. I., & Lin, D. N. C. 2007, ApJ, 661, 1180
pandas development team, T. 2020, pandas-dev/pandas: Pandas, 1.5.0, Zenodo, doi:10.5281/zenodo.3509134
Patra, K. C., Winn, J. N., Holman, M. J., et al. 2017, AJ, 154, 4
Petigura, E. A., Howard, A. W., Marcy, G. W., et al. 2017, AJ, 154, 107
Petrovich, C., Deibert, E., & Wu, Y. 2019, AJ, 157, 180
Petrovich, C., Malhotra, R., & Tremaine, S. 2013, ApJ, 770, 24
Plez, B., 2012 Turbospectrum: Code for spectral synthesis, Astrophysics Source Code Library, ascl:1205.004
Price-Whelan, A. 2018, adrn/pyia: v0.2, Zenodo, doi:10.5281/zenodo.1228136
Queloz, D., Bouchy, F., Moutou, C., et al. 2009, A&A, 506, 303
Ray, R. D., Eanes, R. J., & Lemoine, F. G. 2001, GeoJI, 144, 471
Rebull, L. M., Stauffer, J. R., Cody, A. M., et al. 2018, AJ, 155, 196
Rebull, L. M., Stauffer, J. R., Cody, A. M., et al. 2020, AJ, 159, 273
Riello, M., De Angeli, F., Evans, D. W., et al. 2021, A&A, 649, A3
Rowell, N., Davidson, M., Lindegren, L., et al. 2021, A&A, 649, A11
Sanchis-Ojeda, R., Rappaport, S., Winn, J. N., et al. 2014, ApJ, 787, 47
Sanchis-Ojeda, R., Rappaport, S., Pallè, E., et al. 2015, ApJ, 812, 112
Santana, F. A., Beaton, R. L., Covey, K. R., et al. 2021, AJ, 162, 303
Schlaufman, K. C., Lin, D. N. C., & Ida, S. 2010, ApJL, 724, L53
Shetrone, M., Bizyaev, D., Lawler, J. E., et al. 2015, ApJS, 221, 24
Skrutskie, M. F., Cutri, R. M., Stiening, R., et al. 2006, AJ, 131, 1163
Smith, V. V., Cunha, K., Shetrone, M. D., et al. 2013, ApJ, 765, 16
Smith, V. V., Bizyaev, D., Cunha, K., et al. 2021, AJ, 161, 254
Stassun, K. G., Collins, K. A., & Gaudi, B. S. 2017, AJ, 153, 136
Taylor, M. B. 2005, in ASP Conf. Ser. 347, Astronomical Data Analysis Software and Systems XIV, ed. P. Shopbell, M. Britton, & R. Ebert (San Francisco, CA: ASP), 29
Terquem, C., & Papaloizou, J. C. B. 2007, ApJ, 654, 1110
Tobie, G., Grasset, O., Dumoulin, C., & Mocquet, A. 2019, A&A, 630, A70
Torra, F., Castañeda, J., Fabricius, C., et al. 2021, A&A, 649, A10
Turner, J. D., Ridden-Harper, A., & Jayawardhana, R. 2021, AJ, 161, 72
Vanderburg, A., Becker, J. C., Buchhave, L. A., et al. 2017, AJ, 154, 237
Virtanen, P., Gommers, R., Oliphant, T. E., et al. 2020, NatMe, 17, 261
Vissapragada, S., Chontos, A., Greklek-McKeon, M., et al. 2022, ApJL, 941, L31
Wallenquist, Å. 1950, ArA, 1, 59
Ward, W. R. 1997, Icar, 126, 261
Weinberg, N. N., Arras, P., Quataert, E., & Burkart, J. 2012, ApJ, 751, 136
Weinberg, N. N., Davachi, N., Essick, R., et al. 2024, ApJ, 960, 50
Weinberg, N. N., Sun, M., Arras, P., & Essick, R. 2017, ApJL, 849, L11
Wenger, M., Ochsenbein, F., Egret, D., et al. 2000, A&AS, 143, 9
Wilson, J. C., Hearty, F. R., Skrutskie, M. F., et al. 2019, PASP, 131, 055001
Wu, Y., & Lithwick, Y. 2013, ApJ, 763, 13
Xiang, M., & Rix, H.-W. 2022, Natur, 603, 599
Yee, S. W., Winn, J. N., Knutson, H. A., et al. 2020, ApJL, 888, L5
Yi, S., Demarque, P., Kim, Y.-C., et al. 2001, ApJS, 136, 417
Yi, S. K., Kim, Y.-C., & Demarque, P. 2003, ApJS, 144, 259
Zasowski, G., Johnson, J. A., Frinchaboy, P. M., et al. 2013, AJ, 146, 81
Zasowski, G., Cohen, R. E., Chojnowski, S. D., et al. 2017, AJ, 154, 198
Zeng, L., Jacobsen, S. B., Sasselov, D. D., et al. 2019, PNAS, 116, 9723
Zhao, G., Zhao, Y.-H., Chu, Y.-Q., Jing, Y.-P., & Deng, L.-C. 2012, RAA, 12, 723
Ziegler, C., Tokovinin, A., Briceño, C., et al. 2020, AJ, 159, 19